

# Coercivity and magnetization reversal mechanism in ferromagnet/antiferromagnet bilayers: Correlation with microstructure of ferromagnetic layers

R. Shan,<sup>1</sup> W. W. Lin,<sup>2</sup> L. F. Yin,<sup>1</sup> C. S. Tian,<sup>1</sup> H. Sang,<sup>2</sup> L. Sun,<sup>3</sup> and S. M. Zhou<sup>1,2,\*</sup>

<sup>1</sup>Surface Physics Laboratory (National Key Laboratory), Fudan University, Shanghai 200433, China

<sup>2</sup>National Laboratory of Solid State Microstructures, Nanjing University, Nanjing 210093, China

<sup>3</sup>Department of Mechanical Engineering, University of Houston, Houston, Texas 77204, USA

(Received 9 August 2004; revised manuscript received 27 October 2004; published 8 February 2005)

Exchange biasing in  $\text{Co}_{20}\text{Ni}_{80}/\text{FeMn}$  and  $\text{Co}_{80}\text{Cr}_{20}/\text{FeMn}$  bilayers has been investigated, where the CoCr layers are of granular structure and the CoNi layers are in the form of a single phase. In the above two series of bilayers, the exchange field is proportional to  $1/t_{\text{FM}}$  ( $t_{\text{FM}}$  denotes ferromagnetic layer thickness). For CoNi/FeMn bilayers, the coercivity and the uniaxial anisotropic field decrease with increasing  $t_{\text{FM}}$  with a linear scale of  $1/t_{\text{FM}}$ . Since they are equal to each other, the magnetization reversal process can be described by magnetization coherent rotation and the coercivity enhancement can be explained in terms of a uniaxial anisotropy model. For CoCr/FeMn bilayers, however, the coercivity displays unusual behaviors. First, in comparison with that of single CoCr layer films, the coercivity is *reduced* instead of enhanced. Secondly, it *increases* with increasing  $t_{\text{FM}}$ . Finally, the coercivity of the bilayers is *not* equal to the uniaxial anisotropic field. A noncoherent rotation process is proposed to occur during the magnetization reversal process. The different characteristics of the coercivity and magnetization reversal mechanisms in the two series of bilayers result from the different microstructures in the CoNi and CoCr layers. The present work might be helpful to clarify the mechanism for the coercivity enhancement in ferromagnet/antiferromagnet bilayers.

DOI: 10.1103/PhysRevB.71.064402

PACS number(s): 75.30.Et, 75.30.Gw, 75.60.Jk

## I. INTRODUCTION

For exchange-biased antiferromagnet (AF)/ferromagnet (FM) bilayers, the coercivity  $H_C$  of the pinned FM layers is *usually* enhanced in comparison to that of corresponding free FM layers and the hysteresis loop is shifted away from the zero field, which can be used as a fingerprint of the exchange biasing.<sup>1-3</sup> The exchange field  $H_E$  is inversely proportional to the FM layer thickness. The enhanced  $H_C$  *normally* decreases with increasing FM layer thickness. As being pointed out by a phenomenological model, the  $H_C$  enhancement is related to the anisotropic properties of the AF layers, the interfacial exchange coupling energy, and the domain-wall energy density of FM layers.<sup>4</sup> The quantitative dependence of the  $H_C$  enhancement on the constituent layer thickness is less well understood. For example,  $H_C$  has been found to vary as a linear function of  $1/t_{\text{FM}}$  (where  $t_{\text{FM}}$  is the FM layer thickness) in permalloy/FeMn bilayers while it has a  $1/t_{\text{FM}}^{3/2}$  dependence in permalloy/CoO bilayers.<sup>5,6</sup>

In addition to the factors mentioned above, the intrinsic magnetic properties and the magnetization reversal mechanism of the free FM layers should also have a great influence on the  $H_C$  enhancement.<sup>4,7</sup> Several theoretical models considering these effects have been developed to quantitatively account for the  $H_C$  enhancement.<sup>8-11</sup> For example, Qian *et al.* proposed a so-called uniaxial anisotropy model,<sup>9</sup> in which the  $H_C$  enhancement can be explained in terms of an induced uniaxial anisotropy. Since the uniaxial anisotropy is induced by the interfacial exchange coupling, it should be proportional to  $1/t_{\text{FM}}$ . In the case of the coherent rotation model,  $H_C$  should be equal to the uniaxial anisotropic field and thus is inversely proportional to the FM layer thickness. The linear dependence of the  $H_C$  enhancement on  $1/t_{\text{FM}}$  results

from the coherent magnetization reversal process and the uniaxial anisotropy. In order to explain the  $1/t_{\text{FM}}^{3/2}$  dependence, a random field model was used.<sup>6</sup> In this model, the FM layers are considered to break into multiple domains during the magnetization reversal process, and the AF pinning materials provide additional critical fields, such as interfacial random fields,<sup>8,12</sup> to hinder the motion of the FM domain wall. With the noncoherent magnetization rotation and multidomain formations,  $H_C$  of the exchange-biased layers will be determined by the competition between the critical field of the free FM layers and the additional critical field given by AF materials. If the critical field of the domain-wall motion in the free FM layers is larger than that provided by the AF layers, no coercivity enhancement can be expected. Therefore, the detailed magnetization reversal process is of crucial importance in the explanation of the coercivity enhancement.

From the above analysis, it can be known that the coercivity enhancement in AF/FM bilayers should also depend on the microstructure of corresponding free FM layers since the magnetization reversal form is strongly related to the microstructure of the FM layers. To date, most of the studies about the coercivity enhancement have been focused on AF/FM bilayers with FM materials of single phase such as Co, Fe, permalloy, and CoFe alloys.<sup>3</sup> The intrinsic coercivity and critical field for the motion of domain walls are very small in these materials. In order to study the effect of the microstructure of the FM layers on the coercivity enhancement, more experiments are required with the FM materials of extremely different microstructures. In this paper, we will clearly show that the microstructure has a strong effect on the magnetization reversal process and the coercivity enhancement of the FM/AF bilayers by using  $\text{Co}_{80}\text{Cr}_{20}$

(CoCr)/Fe<sub>50</sub>Mn<sub>50</sub> (FeMn) and Co<sub>20</sub>Ni<sub>80</sub> (CoNi)/FeMn bilayers. As is well known, CoCr alloys as a magnetic recording material possess a granular microstructure and special magnetization reversal mechanism.<sup>13</sup> In contrast, the CoNi alloy is a typical magnetically soft material of single phase.<sup>14</sup> The magnetization reversal mechanism and coercivity enhancement in CoNi/FeMn bilayers are found to be different from those for CoCr/FeMn bilayers.

## II. EXPERIMENTS

Two samples of substrate/Cu (30 nm)/CoCr(0–30 nm) and substrate/Cu(30 nm)/CoCr (0–30 nm)/FeMn (20 nm), which were denoted as CoCr single-layer film and CoCr/FeMn bilayers, were deposited by dc magnetron sputtering on Si(100) from Cu, Co<sub>80</sub>Cr<sub>20</sub>, and Fe<sub>50</sub>Mn<sub>50</sub> targets with deposition rates of about 0.1 nm/s. The base pressure was  $4 \times 10^{-5}$  Pa and the Ar pressure is 0.45 Pa during deposition. Wedge-shaped CoCr layers were used in order to avoid run-to-run error. The 30-nm-thick Cu buffer layer is used to stimulate the (111) growth of fcc FeMn layers, which were finally covered by another 30-nm-thick Cu capping layer. A deposition field of about 130 Oe was applied parallel to the film plane during deposition to establish the exchange biasing in CoCr/FeMn bilayers and uniaxial anisotropy in CoCr single-layer films. No usual field cooling (FC) was performed for the CoCr/FeMn bilayers. Easy axis in CoCr single-layer films and CoCr/FeMn bilayers is parallel to the deposition field. Microstructure characteristic of single thick CoCr films was analyzed by transmission electron microscopy (TEM) and x-ray diffraction.

A large sample of Cu (30 nm)/wedged-Co<sub>20</sub>Ni<sub>80</sub> (0–25 nm)/uniform-FeMn (15 nm) was prepared onto a Si (100) substrate using a dc magnetron sputtering system with a base pressure of  $4 \times 10^{-5}$  Pa. The 30-nm-thick Cu buffer layer was also used to promote the growth of (111) oriented fcc AF FeMn. Details of preparations were similar to those for permalloy/FeMn ones.<sup>5</sup> The unidirectional anisotropy was established by using a standard field-cooling process from 420 K to room temperature under an applied field of 10 kOe parallel to the deposition field.

A vibrating sample magnetometer (VSM) was used to measure in-plane hysteresis loops to determine  $H_E$  and  $H_C$ . Ferromagnetic resonance (FMR) measurements were carried out using a Bruker ER 200D-SRC EPR spectrometer, with a fixed microwave frequency of 9.78 GHz and swept external dc field. The FMR spectra with respect to various orientations of the dc magnetic field  $\vec{H}$  were obtained by changing the azimuthal angle  $\phi_H$  in the film plane. All measurements were carried out at room temperature.

## III. RESULTS AND DISCUSSION

Figure 1 shows the Co jump-ratio imaging of CoCr (20 nm) single-layer films. The TEM plan view bright field micrograph shows composition nonuniformity in the deposited CoCr layer. The granular structure with coexisting Co-rich and Cr-rich phases was commonly observed in CoCr alloys.<sup>13</sup> The Cr-rich phase refers to the CrCo alloy with Cr

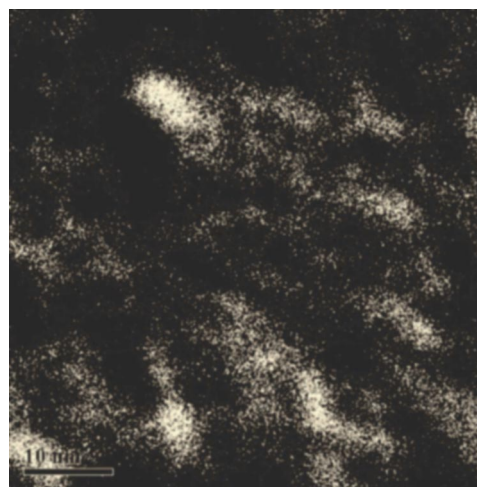


FIG. 1. Co jump-ratio imaging of CoCr (20 nm) single-layer films obtained from electron-energy-loss spectra in TEM. The bright region means a higher Co content than the dark region.

composition higher than 25 at. % and is paramagnetic at room temperature. The Co-rich phase refers to the CoCr alloy with Cr composition lower than 25 at. % and is ferromagnetic at room temperature.<sup>14</sup>

Figure 2 shows the x-ray-diffraction spectrum of CoCr(20 nm)/FeMn (20 nm) bilayers. Apparently, Cu and FeMn layers are of fcc texture with (111) and (220) orientations and the intensity of the former diffraction peak is much stronger than that of the latter one. It is noted that the fcc FeMn is antiferromagnet and is essential to establish the exchange biasing, and the (111) preferred orientation of FeMn layers was argued to have a stronger exchange biasing than other orientations.<sup>3,15</sup> A broad diffraction peak of CoCr(10 $\bar{1}$ 1) exists. Two possible reasons can be proposed to broaden the peak. First, it might mean small grains of CoCr. Small grains and even amorphous structure were observed in as-prepared thin CoCr layer films.<sup>16</sup> Secondly, it is caused by the inhomogeneous distribution of the composition in CoCr layers. This is because the position of the diffraction peak is strongly related to the composition. From Fig. 2, one can find that the grain size of FeMn is much larger than that of CoCr. The exchange biasing can still be established, although a

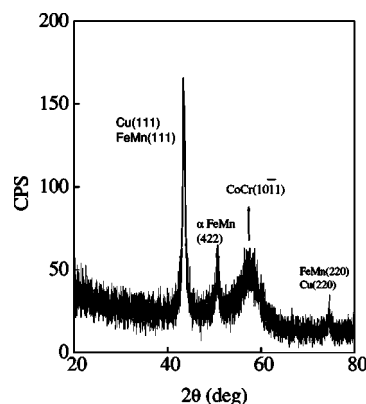


FIG. 2. X-ray-diffraction spectrum of CoCr (20 nm)/FeMn (20 nm) bilayers with a Cu  $K\alpha$  source.

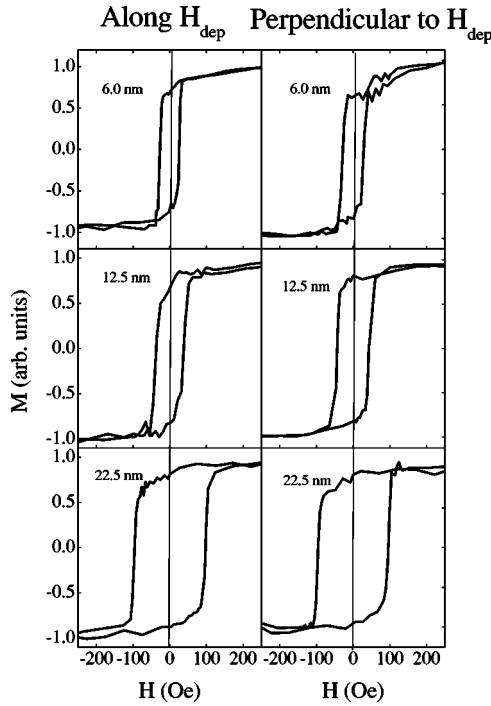


FIG. 3. Typical in-plane hysteresis loops of CoCr single-layer films with different layer thickness along the deposition field  $H_{\text{dep}}$  (left column) and perpendicular to  $H_{\text{dep}}$  (right column). The inset numbers refer to the CoCr layer thickness.

small diffraction peak of  $\alpha$  FeMn is also detected. Moreover, the CoNi layers are in the form of a single phase.<sup>14</sup> Therefore, the microstructures of the CoNi and CoCr layers are extremely different.

Magnetization measurement results of single CoCr layer films are shown in Fig. 3. One can find that the in-plane hysteresis loops are squared for all orientations of the applied magnetic field with respect to the deposition field. Figure 4 shows typical in-plane hysteresis loops of CoCr/FeMn bilayers with various FM layer thickness. Along the easy axis, i.e., the direction of the deposition field, the hysteresis loop is squared for thick CoCr layers but slanted for very thin CoCr layers. For all samples, the hysteresis loops are shifted away from the zero field, demonstrating the introduction of the exchange biasing.  $H_E$  increases with decreasing FM layer thickness. Similar to the CoCr single-layer films,  $H_C$  of the bilayers increases with increasing FM layer thickness. Along the hard axis, the hysteresis loop is completely slanted for small CoCr layer thickness and is almost squared for large CoCr layer thickness. At the same time, the hysteresis loop is centered about the zero magnetic field. After comparing the results in Figs. 3 and 4, one can find that an enhancement of the uniaxial anisotropy has been induced in the CoCr/FeMn bilayers by AF layers.

Figure 5 shows the angular dependence of the in-plane resonance field for CoNi/FeMn and CoCr/FeMn bilayers and CoCr single-layer films. For all CoNi/FeMn bilayers, as shown in Fig. 5(a), the angular dependence can be well described by unidirectional and uniaxial anisotropies. The usual expression for the resonance field can be written as<sup>17,18</sup>

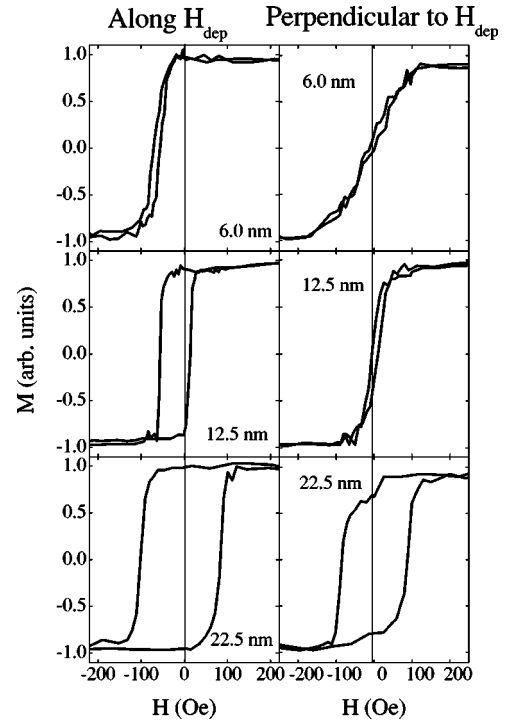


FIG. 4. Typical in-plane hysteresis loops of CoCr/FeMn (20 nm) bilayers with different CoCr layer thickness along the deposition field  $H_{\text{dep}}$  (left column) and perpendicular to  $H_{\text{dep}}$  (right column). The inset numbers refer to the CoCr layer thickness. The easy axis is parallel to the deposition field.

$$H_{\text{res}} = H_0 - H_E^{\text{FMR}} \cos \phi_H - H_K \cos 2\phi_H, \quad (1)$$

where  $\phi_H$  is an azimuthal angle between the external field and the unidirectional axis.  $H_E^{\text{FMR}}$  is the FMR-measured exchange field and the uniaxial anisotropy field  $H_K = 2K_U/M_{\text{FM}}$ , where  $K_U$  and  $M_{\text{FM}}$  are the uniaxial anisotropy energy and the FM magnetization, respectively. The isotropic resonance field shift  $H_0$ , taken as the average value of the in-plane resonance field  $H_{\text{res}}$ , was suggested to come from the irreversible rotation of the AF spins.<sup>18</sup>

For CoCr/FeMn bilayers and CoCr single-layer films with thick FM layers, the unidirectional and uniaxial anisotropic fields can be calculated easily, as shown in Fig. 5(b). With thin FM layers, however, the FMR spectra cannot be fitted just considering the unidirectional and uniaxial anisotropies; additional symmetrical anisotropy terms must be included. For all CoCr layer thickness, the angular-dependent FMR spectra of single CoCr layer and CoCr/FeMn bilayers are similar to each other. The well defined angular dependence of the resonance field in CoNi/FeMn bilayers is related to the single phase of CoNi layers. So, it is indicated that the magnetic anisotropic properties of the FM/AF bilayers are closely related to the microstructure of corresponding FM layers. Moreover, the magnitude of the anisotropic field for CoCr/FeMn bilayers is larger than that of CoCr single-layer films for all CoCr layer thickness and the additional uniaxial anisotropy is therefore induced by the AF layers.

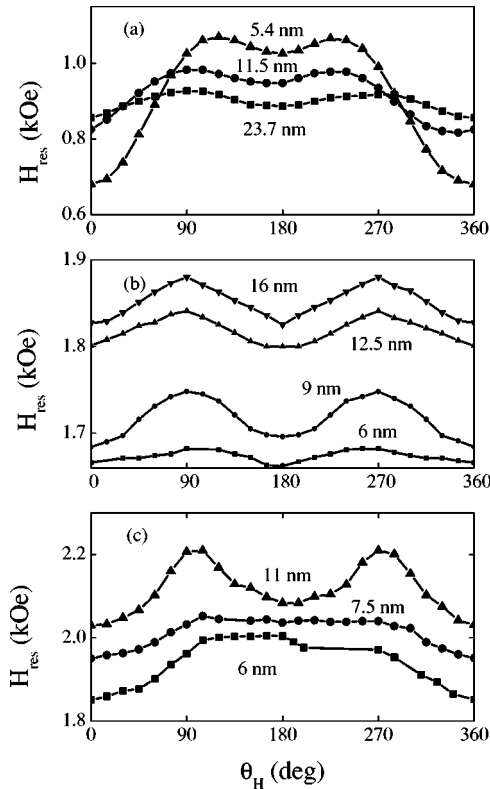


FIG. 5. Typical angular dependence of the in-plane ferromagnetic resonance field for CoNi/FeMn bilayers (a), CoCr single-layer films (b), and CoCr/FeMn bilayers (c). The inset numbers refer to the FM layer thickness.

Figure 6 shows the exchange field in CoNi/FeMn and CoCr/FeMn bilayers. For the two series of samples, the values of  $H_E$  from the VSM and the FMR are equal to each other and are inversely proportional to the FM layer thickness. Obviously, the values of  $H_E$  from the two methods are identical although the CoNi and CoCr layers have different microstructures and magnetization reversal mechanisms, unlike other experimental results.<sup>19,20</sup> Although the CoCr layers have a granular structure, the linear dependence still holds in the CoCr/FeMn bilayers. It is noted that  $H_E$  has a small but negative value as  $1/t_{FM}$  approaches zero, which might be due to a measurement artifact. With the slope of the curve and the FM magnetization, one can calculate the exchange coupling energy. It is  $0.011 \text{ erg/cm}^2$  for CoCr/FeMn bilayers and  $0.057 \text{ erg/cm}^2$  for CoNi/FeMn bilayers. Note that the exchange biasing is established by the deposition field and the post-FC for CoCr/FeMn and CoNi/FeMn bilayers, respectively. For specific FM/AF bilayers, the exchange coupling energy in the case of post-FC is larger than that of as-prepared samples.<sup>21</sup> Other reasons like small magnetization and rough CoCr/FeMn interfaces should also be considered. The magnetization of  $320 \text{ emu/cm}^3$  for CoCr layers is about half of the value of  $640 \text{ emu/cm}^3$  for permalloy alloys. Since the exchange coupling energy scales as a function of  $\sqrt{M_{FM}}$ ,<sup>22</sup> the small magnetization of the CoCr layer is another major reason for small exchange coupling energy. Moreover, the granular structure of the CoCr layers is expected to have a great impact on the interface roughness, the

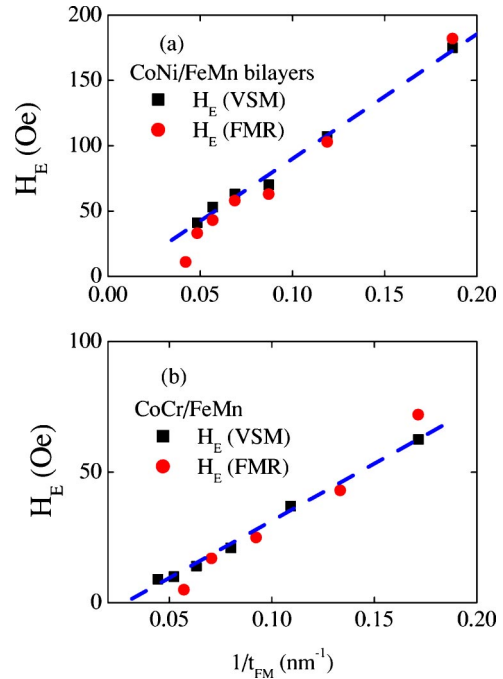


FIG. 6. Dependence of  $H_E$  on the FM layer thickness for CoNi/FeMn (a) and CoCr/FeMn (b) bilayers. The values of the exchange field were obtained by VSM and FMR. The dashed lines refer to linear fit results.

microstructure of the FeMn layers, and thus the exchange coupling energy.<sup>13</sup>

Figure 7 shows the variations of the  $H_C$  and the anisotropic field versus the FM layer thickness for CoNi/FeMn and CoCr/FeMn bilayers, and CoCr single thick films. As shown in Fig. 7(a), for CoNi/FeMn bilayers, the coercivity

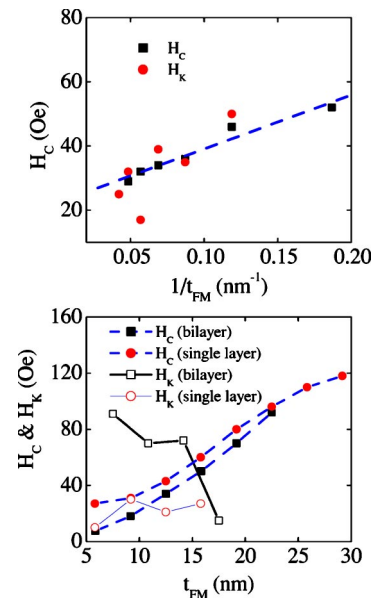


FIG. 7. Dependence of  $H_C$  and the anisotropic field  $H_K$  on the FM layer thickness for CoNi/FeMn bilayers (a), and the CoCr single-layer films and CoCr/FeMn bilayers (b). The dashed line in (a) refers to a linear fit.

and the anisotropic field are equal to each other and both of them are proportional to the inverse FM layer thickness, demonstrating an interfacial nature. Apparently, the coercivity enhancement can be attributed to the induced uniaxial anisotropy and the magnetization reversal process can be described by the coherent rotation model. Therefore, for CoNi/FeMn bilayers, the coercivity behavior can be explained very well by the uniaxial anisotropy model.<sup>9</sup> Similar results were also observed in permalloy/FeMn bilayers.<sup>18</sup>

It is well known that for CoCr single-layer films,  $H_C$  shows strong microstructure dependence.<sup>13</sup> As shown in TEM micrograph (Fig. 1), the CoCr layer consists of Co-rich and Cr-rich phases and the former grains are separated by the latter ones. For small CoCr layer thickness, the  $c$  axis of the hcp Co-rich component is distributed in the film plane randomly,<sup>16</sup> which results in isotropic in-plane hysteresis loops in Fig. 3. For CoCr single-layer films, two important factors have influence on the dependence of  $H_C$  on the FM layer thickness, including the size of Co-rich grains and their interaction. As the CoCr layer thickness is increased, the grain size of the Co-rich component increases.<sup>23</sup> As shown in Figs. 1 and 2, the grain size is as small as a few nanometers and much smaller than the critical value for single domain particles. In this case,  $H_C$  should increase as the grain size and thus the CoCr layer thickness are increased. At the same time, the separation between Co-rich grains increases with increasing CoCr layer thickness and the interaction becomes weak accordingly. This favors coherent rotation in individual Co-rich grains and thus coercivity enhancement.<sup>24</sup> The variation of  $H_C$  in CoCr single-layer films with increasing the CoCr layer thickness can be clearly understood.

For CoCr single-layer films, the hysteresis loops are almost isotropic with respect to the external magnetic field, which does not coincide with the angular dependence of the in-plane resonance field, as shown in Figs. 3 and 5. At the same time, the coercivity is not equal to the anisotropic field, as shown in Fig. 7(b). Therefore, the magnetization reversal of the CoCr single-layer films is accompanied by the noncoherent rotation model and  $H_C$  is determined by the critical field during the motion of the domain wall. Note that 180 degree domain walls were observed in thin CoCr layers.<sup>25</sup> As discussed above, the magnetization reversal process of all CoCr single-layer films is related to the granular microstructure of CoCr layers.

As shown in Fig. 7(b), the uniaxial anisotropic field in CoCr/FeMn bilayers is enhanced, in comparison with CoCr single-layer films. The anisotropic field in CoCr/FeMn bilayers decreases with increasing FM layer thickness but does not change significantly with FM layer thickness in CoCr single-layer films. The enhancement of the uniaxial anisotropy in CoCr/FeMn bilayers decreases with increasing FM layer thickness and can therefore be ascribed to the exchange coupling between CoCr and FeMn bilayers, demonstrating an interfacial nature. As shown in Fig. 7(b), however, for CoCr/FeMn bilayers and CoCr single-layer films, the  $H_C$  increases with increasing CoCr layer thickness. More importantly,  $H_C$  of the CoCr/FeMn bilayers is smaller than that of CoCr layers, that is to say,  $H_C$  is *reduced instead of enhanced*. The reduction decreases with increasing CoCr layer thickness. These distinguished features are contrary to results

for CoNi/FeMn bilayers and other conventional ones.<sup>3</sup> As shown in Fig. 7, one can find that the uniaxial anisotropic field and the coercivity are not equal to each other for most of the CoCr/FeMn bilayers. Apparently, the coercivity behavior and the magnetization reversal process in CoCr/FeMn bilayers cannot be explained in terms of the uniaxial anisotropy model and the magnetization coherent rotation model.<sup>9</sup> The magnetic properties of CoCr/FeMn bilayers are in agreement with those of CoCr single-layer films.

The reason for the reduction of the  $H_C$  in the CoCr/FeMn bilayers in comparison with free CoCr layers can be explained as follows. As an AF material, the FeMn layers have two effects on  $H_C$  of the CoCr layers. First, the FeMn layer has a pinning effect on the CoCr layer. Since the coercivity behavior in CoCr/FeMn bilayers cannot be attributed to the uniaxial anisotropy model,<sup>9</sup> other models like the random field or interfacial magnetic frustration must be considered to explain the phenomena.<sup>8,10</sup> New critical fields given by FeMn layers might also hinder the motion of the domain wall in CoCr layers. If the new critical fields are not larger than the intrinsic ones of the CoCr layers,  $H_C$  of the CoCr/FeMn bilayers is not larger than that of the CoCr single-layer films and consequently no coercivity enhancement occurs. According to the random field model,<sup>6</sup> the critical field is proportional to  $\sqrt{J_{\text{FM-AF}}}$ . Since  $J_{\text{FM-AF}}$  is the average exchange coupling energy at the FM/AF interface and is strongly related to the interfacial roughness, it is not easy to obtain the value of  $J_{\text{FM-AF}}$ . Therefore, the critical field cannot be obtained without the exact value of  $J_{\text{FM-AF}}$ . Alternatively, however, since the exchange biasing in the present CoCr/FeMn bilayers is so weak that the exchange coupling energy is as small as 0.011 erg/cm<sup>2</sup>, one can predict that the interfacial interaction is weak and thus the critical field is very small. This conjecture needs further experimental investigation. At least one can know that the coercivity enhancement is equal to zero or very small because of the weak exchange coupling energy.

The second effect of the FeMn layers originates from additional interactions between Co-rich grains in the bilayers. Since the grain size of FeMn is much larger than that of CoCr, the neighboring grains of CoCr can be connected to each other through FeMn grains and the Co-rich grains in CoCr/FeMn bilayers are further coupled to each other through the FeMn ones, in addition to the interaction through the Cr-rich component. The mechanism of the interaction is similar to the interlayer coupling between FM layers in FM/AF/FM sandwiches or multilayers.<sup>26</sup> Therefore, the average interaction between CoCr grains becomes stronger than that of the single-layer films and  $H_C$  of bilayers becomes smaller than that of CoCr free layer films.<sup>23</sup> From the above analysis, the FeMn layers have two impacts on the coercivity characteristic of the CoCr/FeMn bilayers. Unfortunately, they are difficult to be separated from each other since the two effects exist simultaneously. These effects become weak with increasing CoCr layer thickness and the difference of the coercivity between the bilayers and the single-layer films approaches zero, as shown in Fig. 7(b).

It is instructive to compare our specific system with the generally observed coercivity enhancement in granular

FM/AF systems.<sup>1,27</sup> Two major reasons can be used to explain the difference in exchange biasing between these two configurations. First, in Co/CoO and Co/NiO powder system, the inner Co is of single phase while the CoCr layer in our system is of two phases, which might induce different magnetization reversal mechanisms. Secondly, no dipolar interaction exists between Co powders while it exists in CoCr/FeMn bilayers. Moreover, the pinning effect of the CoO and NiO coating layers is different from that of the FeMn layers. Studies of the exchange biasing in FM/AF bilayers with granular configuration will be helpful to reveal the nature of the coercivity enhancement because a different magnetization reversal mode can be obtained by modifying the shape and the size of granules.

#### IV. CONCLUSIONS

Magnetic properties of sputtered CoNi/FeMn bilayers, CoCr/FeMn bilayers, and CoCr single-layer films have been studied. For exchange-coupled CoNi/FeMn and CoCr/FeMn bilayers,  $H_E$  is proportional to the inverse FM layer thickness. For CoNi/FeMn bilayers, the coercivity and the anisotropic field are equal to each other and both decrease with increasing FM layer thickness as a linear scale of  $1/t_{FM}$ . For most of the CoCr/FeMn bilayers,  $H_C$  is smaller than that of

the CoCr single-layer films and increases with increasing  $t_{FM}$  in the two series of samples. For CoCr/FeMn bilayers, the coercivity differs from the anisotropic field. The magnetization reversal process can be described by the coherent rotation model in CoNi/FeMn bilayers while it is accompanied by a noncoherent rotation process in CoCr/FeMn bilayers. The uniaxial anisotropy model can be employed to explain the coercivity enhancement in CoNi/FeMn bilayers. Other models must be considered to explain the usual coercivity behavior in CoCr/FeMn bilayers, in which the detailed magnetization reversal mechanism should be considered. These results indicate that the coercivity and the magnetization reversal mechanism of the FM layers are related to the microstructure of the FM layers. The present work might be helpful to clarify the mechanism of the coercivity enhancement in FM/AF bilayers.

#### ACKNOWLEDGMENTS

This work was supported by the National Science Foundation of China (Grants No. 10174014, No. 60271013, No. 10321003, No. 10021001, and No. 60490290), the State Key Project of Fundamental Research (Grants No. 2001CB610602 and No. 2002CB613504), and JSNSF. The authors would like to thank Z. M. Jiang at Fudan University for the x-ray measurements.

\*Correspondence author. Electronic address: shimingzhou@yahoo.com

<sup>1</sup>W. H. Meiklejohn and C. P. Bean, Phys. Rev. **102**, 1413 (1956).

<sup>2</sup>W. H. Meiklejohn and C. P. Bean, Phys. Rev. **105**, 904 (1957).

<sup>3</sup>See, e.g., J. Nogues and I. K. Schuller, J. Magn. Magn. Mater. **192**, 203 (1999).

<sup>4</sup>J. Geshev, L. G. Pereira, and J. E. Schmidt, Phys. Rev. B **66**, 134432 (2002).

<sup>5</sup>S. M. Zhou, K. Liu, and C. L. Chien, Phys. Rev. B **58**, R14 717 (1998).

<sup>6</sup>S. Zhang, D. V. Dimitrov, G. C. Hidjipanayis, J. W. Cai, and C. L. Chien, J. Magn. Magn. Mater. **198–199**, 468 (1999).

<sup>7</sup>L. Wang, B. You, S. J. Yuan, J. Du, W. Q. Zou, A. Hu, and S. M. Zhou, Phys. Rev. B **66**, 184411 (2002).

<sup>8</sup>L. Zhang and S. Zhang, Phys. Rev. B **61**, R14 897 (2000).

<sup>9</sup>Z. Qian, J. M. Sivertsen, and J. H. Judy, J. Appl. Phys. **83**, 6825 (1998).

<sup>10</sup>C. Leighton, J. Nogués, B. J. Jösso-Åkerman, and Ivan K. Schuller, Phys. Rev. Lett. **84**, 3466 (2000).

<sup>11</sup>M. D. Stiles and R. D. McMichael, Phys. Rev. B **63**, 064405 (2001).

<sup>12</sup>A. P. Malozemoff, J. Appl. Phys. **63**, 3874 (1988).

<sup>13</sup>D. Weller and M. F. Doerner, Annu. Rev. Mater. Sci. **30**, 611 (2000) and references therein.

<sup>14</sup>See, e.g., *Magnetic Properties of Metals*, in *Data in Science and Technology*, edited by H. P. J. Wijn (Springer-Verlag, New York, 1991), p. 38.

<sup>15</sup>R. Nakatan, K. Hoshino, S. Noguchi, and Y. Sugita, Jpn. J. Appl. Phys., Part 1 **33**, 133 (1994).

<sup>16</sup>B. G. Demczyk, Ultramicroscopy **47**, 425 (1992).

<sup>17</sup>M. Rubinstein, P. Lubitz, and S. F. Cheng, J. Magn. Magn. Mater. **195**, 299 (1999).

<sup>18</sup>S. M. Zhou, S. J. Yuan, L. Wang, M. Lu, J. Du, A. Hu, and J. T. Song, Appl. Phys. Lett. **83**, 2013 (2003).

<sup>19</sup>H. Xi, M. White, and S. M. Rezende, Phys. Rev. B **60**, 14 837 (1999).

<sup>20</sup>J. Geshev, Phys. Rev. B **62**, 5627 (2000).

<sup>21</sup>H. Sang, Y. W. Du, and C. L. Chien, J. Appl. Phys. **85**, 4931 (1999).

<sup>22</sup>S. M. Zhou and C. L. Chien, Phys. Rev. B **63**, 104406 (2001).

<sup>23</sup>I. L. Sanders, T. Yogi, J. K. Howard, S. E. Lambert, G. L. Gorman, and C. Hwang, IEEE Trans. Magn. **25**, 3869 (1989).

<sup>24</sup>M. Kitada and N. Shimizu, J. Appl. Phys. **54**, 7089 (1983).

<sup>25</sup>B. G. Demczyk, IEEE Trans. Magn. **28**, 998 (1992).

<sup>26</sup>Z. Y. Liu and S. Adenwalla, Phys. Rev. Lett. **91**, 037207 (2003).

<sup>27</sup>J. Sort, J. Nogués, X. Amils, S. Suriñach, J. S. Muñoz, and M. D. Baró, Appl. Phys. Lett. **75**, 3177 (1999).